Gradual soil water depletion results in reversible changes of gene expression, protein profiles, ecophysiology and growth performance in populus euphratica, a poplar growing in arid regions

Marie-Béatrice Bogeat-Triboulot, Mikael Brosché, Jenny Renaut, Laurent Jouve, Didier Le Thiec, Payam Fayyaz, Basia Vinocur, Erwin Witters, Kris Laukens, Thomas Teichmann, et al.

Gradual Soil Water Depletion Results in Reversible Changes of Gene Expression, Protein Profiles, Ecophysiology, and Growth Performance in *Populus euphratica*, a Poplar Growing in Arid Regions[1][W][OA]

Marie-Béatrice Bogeat-Triboulot[2]*, Mikael Brosché[2], Jenny Renaut[2], Laurent Jouve[2], Didier Le Thiec, Payam Fayyaz, Basia Vinocur, Erwin Witters, Kris Laukens, Thomas Teichmann, Arie Altman, Jean-François Hausman, Andrea Polle, Jaakko Kangasjärvi, and Erwin Dreyer

Institut National de la Recherche Agronomique Nancy, Unité Mixte de Recherche 1137 Institut National de la Recherche Agronomique-Université Henri Poincaré Ecologie et Ecophysiologie Forestières, Institut Fédératif de Recherche 110 Génomique, Ecophysiologie et Ecologie Fonctionnelle, F–54280 Champenoux, France (M.-B.B.-T., D.L.T., E.D.); Plant Biology, Department of Biological and Environmental Sciences, University of Helsinki, FIN–00014 Helsinki, Finland (M.B., J.K.); Centre de Recherche Public-Gabriel Lippmann, Cellule de Recherche en Environnement et Biotechnologies, L–4422 Belvaux, Grand-Duché de Luxembourg (J.R., L.J., J.-F.H.); Institut für Forstbotanik, Georg-August-Universität Göttingen, 37077 Goettingen, Germany (P.F., T.T., A.P.); Robert H. Smith Institute of Plant, Sciences and Genetics in Agriculture, Hebrew University of Jerusalem, Faculty of Agricultural, Food and Environmental Quality Sciences, Rehovot 76100, Israel (B.V., A.A.); and Laboratory of Plant Biochemistry, Department of Biology (E.W., K.L.), and Center for Proteome Analysis and Mass Spectrometry (E.W., K.L.), University of Antwerp, B–2020 Antwerp, Belgium

The responses of *Populus euphratica* Oliv. plants to soil water deficit were assessed by analyzing gene expression, protein profiles, and several plant performance criteria to understand the acclimation of plants to soil water deficit. Young, vegetatively propagated plants originating from an arid, saline field site were submitted to a gradually increasing water deficit for 4 weeks in a greenhouse and were allowed to recover for 10 d after full reirrigation. Time-dependent changes and intensity of the perturbations induced in shoot and root growth, xylem anatomy, gas exchange, and water status were recorded. The expression profiles of approximately 6,340 genes and of proteins and metabolites (pigments, soluble carbohydrates, and oxidative compounds) were also recorded in mature leaves and in roots (gene expression only) at four stress levels and after recovery. Drought successively induced shoot growth cessation, stomatal closure, moderate increases in oxidative stress-related compounds, loss of CO_2 assimilation, and root growth reduction. These effects were almost fully reversible, indicating that acclimation was dominant over injury. The physiological responses were paralleled by fully reversible transcriptional changes, including only 1.5% of the genes on the array. Protein profiles displayed greater changes than transcript levels. Among the identified proteins for which expressed sequence tags were present on the array, no correlation was found between transcript and protein abundance. Acclimation to water deficit involves the regulation of different networks of genes in roots and shoots. Such diverse requirements for protecting and maintaining the function of different plant organs may render plant engineering or breeding toward improved drought tolerance more complex than previously anticipated.

Drought is one of the most important constraints limiting the growth of plants and ecosystem productivity around the world (Passioura, 1996; Aussenac, 2000). Plant responses to water deficit are complex and encompass many aspects, including stress sensing and signaling, changes in growth and biomass allocation patterns, water status homeostasis, decreased stomatal conductance and CO_2 assimilation, osmoregulation, and detoxification processes (Passioura, 1996; Chaves et al., 2003). The impacts of water shortage on plant physiology are numerous and can be assessed at different spatial scales, ranging from the canopy to molecular processes. Approaches at finer scales are expected to improve the understanding of the processes recorded at larger scales. For instance, the biophysics of drought-induced

reduction of cell expansion (Boyer et al., 1985; Cosgrove, 1987) and, at the molecular scale, identification of key genes involved in drought-induced cell wall stiffening (Cosgrove, 2000; Sharp et al., 2004), will contribute to the understanding of the loss of productivity recorded at the organism and ecosystem scales. Moreover, they may help to select genotypes with an improved ability to cope with drought in the future (Vinocur and Altman, 2005; Polle et al., 2006).

Several recent studies have dealt with molecular responses to water shortage (Kreps et al., 2002; Salekdeh et al., 2002; Seki et al., 2002; Xiong and Zhu, 2002; Bray, 2004; Kawaguchi et al., 2004; Vera-Estrella et al., 2004; Hajheidari et al., 2005). However, our knowledge of drought responses in plants is still fragmentary, because previous studies have focused mainly on short-term responses to acute stress rather than on long-term acclimation processes to moderate and gradually increasing water deficits. While short-term studies provide useful information about water deficit sensing and signaling pathways, long-term studies may shed light on genes and/or proteins involved in long-term responses to water deficit and in potential acclimation to low water availability.

In the case of soil water deficit, as opposed to many other abiotic constraints, the time course of water depletion is of central importance, as it may be an effective response modulator in addition to the intensity of the deficit. Indeed, slowly developing soil water depletion usually has physiological consequences that are different from rapid tissue dehydration and possibly implicates different gene networks (Chaves et al., 2003). Up to now, gene expression has been analyzed in plant tissues after exposure to one level of water deficit and/or to short-term dehydration (Kreps et al., 2002; Ozturk et al., 2002; Seki et al., 2002). Furthermore, the impact of water deficit at the proteome level remains relatively unknown and has been restricted to a single level of stress intensity (Salekdeh et al., 2002; Hajheidari et al., 2005; Blödner et al., 2007; Plomion et al., 2006). Gradual soil water depletion is the most common situation for drought in the field and in natural ecosystems. At the whole plant scale, the sequence of events during gradual soil water depletion is well characterized. It usually begins with shoot growth cessation, followed by decreased stomatal conductance, leading in turn to a reduced net CO_2 assimilation rate, impaired photosynthesis, solute accumulation in cells, root growth cessation, and finally, when water availability is very low, induction of leaf senescence and of plant decline (for review, see Passioura, 1996). The changes in transcript and protein profiles underlying the gradual steps of such acclimation processes have received little attention to date.

The genus Populus is an obvious choice for analyzing the responses and acclimation processes occurring during soil water depletion in a tree species, due to the numerous genomic tools that have become available during the last few years (Tuskan et al., 2004). Poplars are known to be drought sensitive (Tschaplinski et al.,

1994; Dreyer et al., 2004), so their natural distribution area is mainly restricted to riparian zones (Bruelheide et al., 2003; Rood et al., 2003). However, some diversity occurs among species and clones with respect to water use efficiency and drought tolerance (Tschaplinski et al., 1994, 1998; Brignolas et al., 2000; Monclus et al., 2006). *Populus euphratica* Oliv. differs considerably from other species of the genus. It grows in semiarid areas and has a strong tolerance to salinity (Sharma et al., 1999; Chen et al., 2003; Gries et al., 2003). Laboratory studies showed that it is able to cope with osmotic stress imposed by NaCl and mannitol (Watanabe et al., 2000; Gu et al., 2004). However, its xylem vessels are among the most vulnerable to drought-induced cavitation (Hukin et al., 2005), suggesting that *P. euphratica* is not intrinsically tolerant to soil water deficit. It is believed that *P. euphratica* is a phreatophyte, able to access deep water, and that its growth rate depends on the depth of the water table (Gries et al., 2003). In an earlier study, we sequenced around 14,000 expressed sequence tags (ESTs) representing genes involved in abiotic stress responses from several normalized and subtracted cDNA libraries produced from control, stress-exposed, and desert-grown *P. euphratica* trees (Brosché et al., 2005). On this basis, a microarray with a unigene set of 6,340 ESTs enriched in stress-related genes was constructed (Brosché et al., 2005) and used in this study to characterize transcriptional responses to gradual soil water depletion. The changes in gene expression were determined at defined stages of water deficit, together with proteomic and physiological alterations and selected stress-related metabolites, to provide a comprehensive analysis of drought acclimation and recovery in Poplar.

RESULTS

Growth, Water Relations, and Gas Exchange in Relation to Water Availability

Young clonal plants of *P. euphratica* were exposed to gradually increasing soil water depletion for about 4 weeks and were fully reirrigated afterward. The soil water content was monitored continuously and was stable through the addition of controlled amounts of water for 3 d prior to sampling (Supplemental Fig. S1). Harvests H1, H2, H3, and H4 were respectively conducted at 35%, 24%, 13%, and 8% relative extractable soil water (soil-REW; Supplemental Fig. S1A; Table I). Harvest H5 was conducted 10 d after full reirrigation.

Decline of stem diameter increment was the first detected effect of soil water depletion (Fig. 1A). It started as soon as soil-REW dropped below 60%, while stem elongation declined at later stages (Fig. 2A; Supplemental Fig. S2). Anatomical analyses of the xylem adjacent to cambium showed that vessel and fiber lumen cross-sectional areas were reduced (Fig. 3, A and B). The decrease in lumen cross-sectional area was accompanied by an increase in vessel density and a

**Table I.** *Summary of key dates during the soil water depletion experiment*

| Day	Time Point/Harvest	Stress Level of Harvested Plants
1	Start	
11	Harvest H1	Control and 35% Soil-REW (10% SWC)
16	Harvest H2	Control and 24% Soil-REW (7.5% SWC)
22	Harvest H3	Control and 13% Soil-REW (5% SWC)
26, 29, and 32	Harvest H4	Control and 8% Soil-REW (4% SWC)
26	Rewatering of plants of batch H5	
36	Harvest H5	Control and reirrigated plants (100% soil-REW)

small decrease in fiber density (vessels per fiber per millimeter; data not shown). Reirrigation resulted in the resumption of diameter growth, with an almost full return to predeficit vessel and fiber diameters. This demonstrated that the effect of soil water deficit on cambial activity was reversible. Parallel to reductions in cell lumen size, a significant increase in the thickness of fiber cell walls was recorded (Fig. 3C).

Stem elongation was reduced when soil-REW dropped below 50%, whereas fine root growth was maintained until soil-REW fell below 20% (Fig. 2A; Supplemental Fig. S2). Stomatal conductance to water vapor (g_s) decreased when soil-REW fell below 40%, before relative leaf water content (RWC) began to decrease (Figs. 1 and 2; Supplemental Fig. S3). Net CO_2 assimilation rate (A) was maintained close to the control level until soil-REW fell below 25%, i.e. long after the onset of stomatal closure. The time lag between the decrease of net CO_2 assimilation rate and that of stomatal conductance demonstrated that *P. euphratica* leaves operated at low instant water use efficiency under conditions of optimal water availability and that water deficit-induced stomatal closure increased it substantially. Reirrigation resulted in a recovery of

Figure 1. Level of physiological functions in drought-stressed *P. euphratica* (relative to controls) as a function of time. A, Growth (diameter, height, and fine roots), net CO_2 assimilation rate (A), and g_s were expressed as a percentage of controls. Sigmoidal curves were adjusted to the data ($y = 100/[1 + \exp\{-(x - x_0)/b\}]$), and correlation coefficients r^2 were 0.90, 0.89, 0.38, 0.78, and 0.95, respectively. B, Ψ_{pd}, Ψ_{md}, and RWC were expressed as the difference between drought stressed and controls. Arrows indicate the five harvest dates (H1–H5). Drought-stressed plants were under controlled irrigation until day 29, while the batch of drought-stressed, reirrigated plants were under controlled irrigation until day 26 and then fully reirrigated.
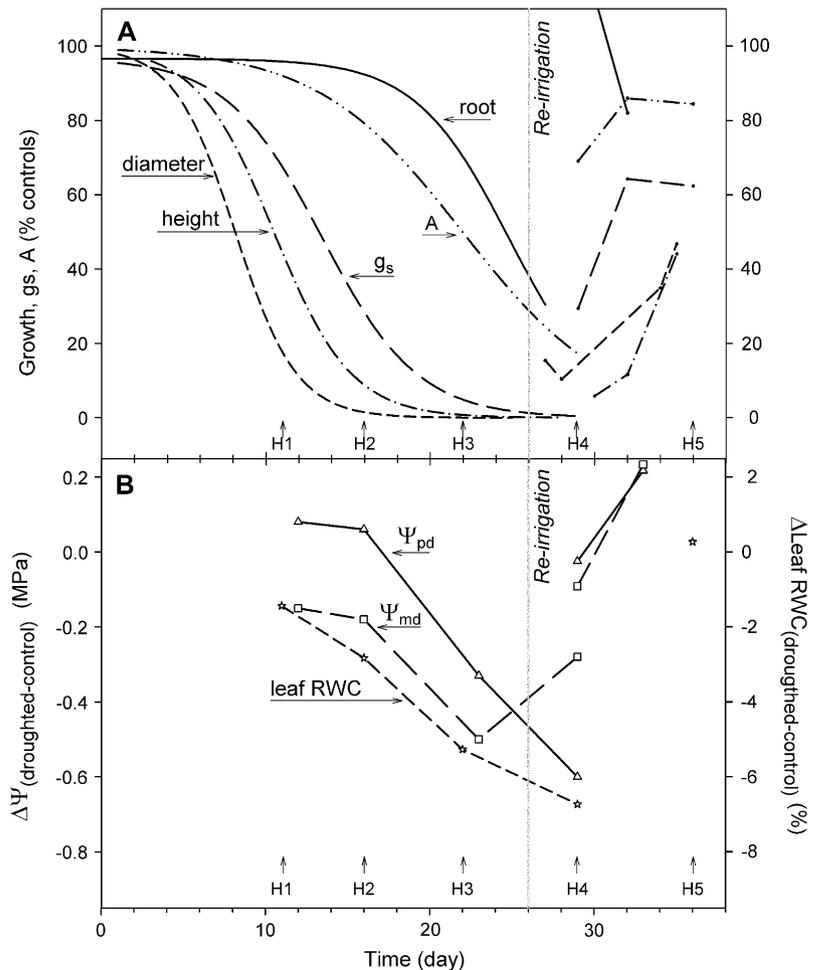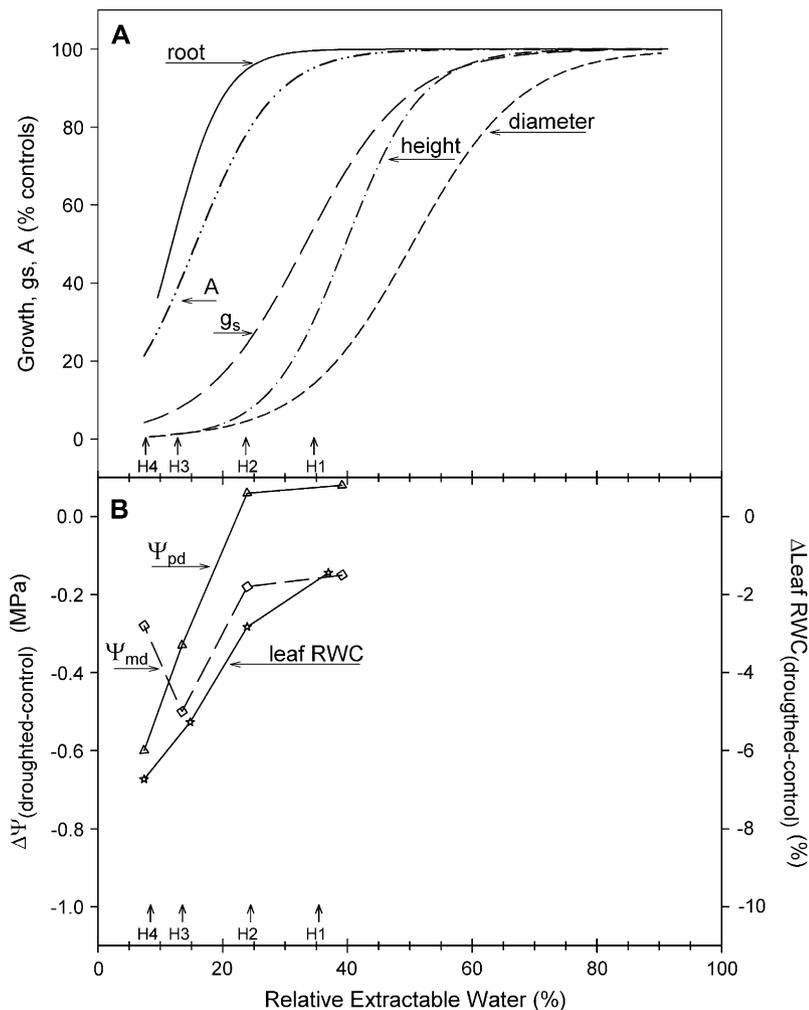
Figure 2. Level of physiological functions in drought-stressed *P. euphratica* (relative to controls) as a function of soil-REW. A, Growth (diameter, height, and fine roots), net CO_2 assimilation rate (*A*), and g_s were expressed as percent of controls. Sigmoidal curves were adjusted to the data ($y = 100/[1 + \exp\{-(x - x_0)/b\}]$), and correlation coefficients r^2 were 0.90, 0.91, 0.38, 0.80, and 0.94, respectively. B, Ψ_{pd}, Ψ_{md}, and RWC were expressed as the difference between drought stressed and controls. Arrows indicate the soil-REW reached at the first four harvest dates (H1–H4).

these activities at levels varying between 60% and 90% of the control levels (Fig. 1).

Predawn leaf water potential (Ψ_{pd}) was a poor index of the changes in water availability, because it was the latest to be affected out of all the recorded parameters (Fig. 1B). Ψ_{pd} of controls was −0.35 MPa, and it decreased only when soil-REW fell below 20% (Fig. 2B). In contrast, midday leaf water potential (Ψ_{md}) was reduced earlier, when soil-REW was still 40% (Figs. 1B and 2B). After a decrease related to soil water depletion (until soil-REW was 15%), Ψ_{md} recovered partially although soil-REW decreased further, and this was due to transpiration cessation induced by almost complete stomatal closure. RWC of controls was 96%. It decreased by less than 2% when soil-REW was reduced to 40% and by only 8% at the peak stress level (Figs. 1B and 2B).

Characterization of Water Stress Levels

These responses to soil water depletion are indices of the intensity of stress undergone by the plants when harvested for metabolic and molecular analyses (Table

I). At harvest H1, plants were submitted to a moderate level of stress resulting in reduced shoot growth (diameter and elongation) and stomatal conductance and in only slightly reduced RWC and Ψ_{md}. The maintenance of root growth led to an increase in the root-to-shoot ratio, a well-known response to mild water deficit, contributing to the maintenance of plant water status through improved/stabilized water uptake capacity at constant or decreasing transpiration. At harvest H2, the plants displayed reduced stomatal conductance and larger intrinsic water use efficiency due to the maintenance of large net CO_2 assimilation rates. Root growth was still active, while shoot growth stopped almost completely. At H3, plants were stressed; Ψ_{pd}, leaf RWC, CO_2 assimilation, and root growth showed significant decline. At H4, plants suffered very severe stress (shoot growth and transpiration stopped completely; photosynthesis, leaf RWC, and root growth decreased strongly), and this even led to senescence symptoms such as yellowing and shedding of older leaves.

Stressed *P. euphratica* plants were able to recover functionality after 10 d of reirrigation (Fig. 1; Supplemental
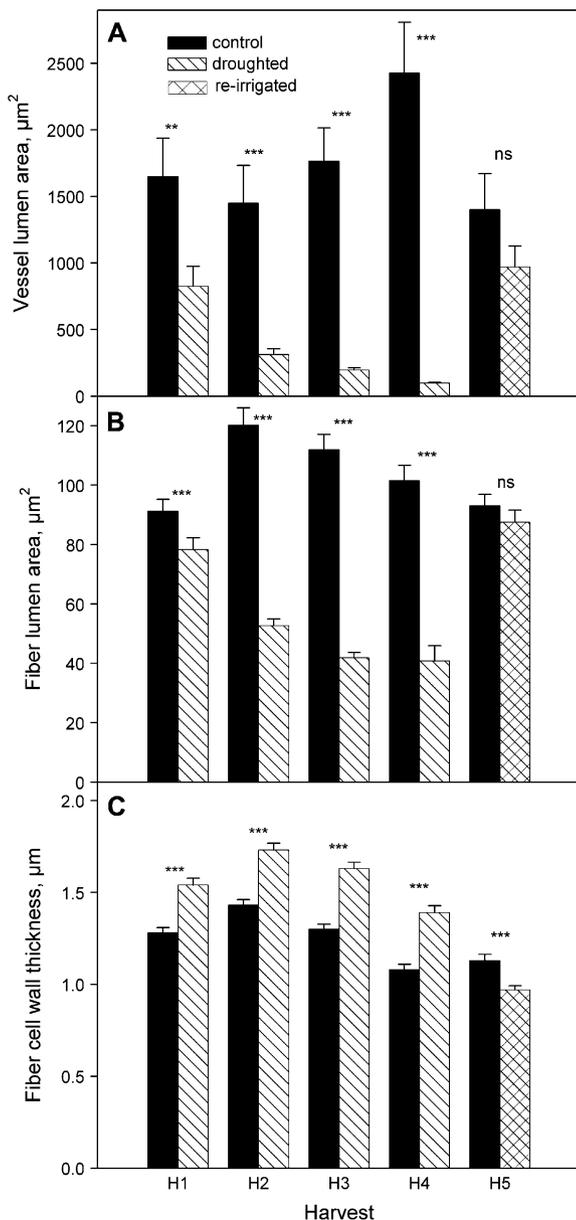
Figure 3. Lumen area of xylem vessels (A) and fibers (B) and fiber cell wall thickness (C) as recorded in stems of *P. euphratica* during water deficit at the five harvest dates. H1 to H4 correspond to four harvest points with increasing soil water depletion and H5 to the harvest after 10 d of reirrigation. Data were recorded in the youngest 100-μm xylem tissue (close to cambium) on two to four plants per harvest and treatment. Mean $\pm$ SE; vessels, $n = 9$ to 95; fibers, $n = 22$ to 369; cell walls, $n = 12$ to 60. *, **, and ***, Difference was significant with $P < 0.05$, $P < 0.01$, and $P < 0.001$, respectively; ns, No significant difference.

Figs. S2 and S3). Stem growth, root growth, stomatal conductance, net CO_2 assimilation, and Ψ (Ψ_p and Ψ_{md} values), respectively, returned to 60%, 80%, 60%, 80%, and 100% of the controls. Growth would probably have recovered completely a few days later, as can be extrapolated from the slope of the growth curves (Fig. 1). Stomatal conductance and photosynthesis reached a plateau 6 d after reirrigation, which may reflect a durable

acclimation induced by the drought episode (improved instant water use efficiency).

Metabolites

The effects of water deficit were also recorded at the metabolite level in leaves. Chlorophyll and carotenoid contents per leaf area were not affected by soil water depletion in mature nonsenescent leaves (harvested from the upper part of the plant; data not shown), but the chlorophyll *a*-to-chlorophyll *b* ratio was significantly increased (Fig. 4). This effect was fully reversed after reirrigation.

Reactive oxygen species (ROS), which occur under stress (Noctor and Foyer, 1998; Mittler, 2002), lead to the oxidation of unsaturated fatty acids in membranes yielding lipid hydroperoxides (LOOH; Taylor et al., 2004). LOOH and malonedialdehyde (MDA), a breakdown product resulting from lipid peroxidation, were used as indices for the occurrence of oxidative stress. No direct correlation was found between water deficit level and LOOH or MDA. While MDA concentrations increased at moderate (H1 [$P = 0.06$] to H3) and not high (H4) stress levels, LOOH concentrations increased at H2 and also after reirrigation (Fig. 4). Because the observed increases in these products of oxidative stress were moderate, we concluded that severe membrane injury did not occur.

To analyze the relationship between detoxification pathways and their products, the ratios of MDA and LOOH from stressed relative to nonstressed plants were plotted against the relative transcript abundance of aldehyde dehydrogenase (AlDH), an enzyme involved in the detoxification of products of lipid peroxide metabolism (Bartels and Souer, 2003; Fig. 5). Increases in AlDH transcript abundance under stress initially correlated with increasing concentrations of MDA. This suggests that the moderate induction of AlDH was insufficient to maintain cellular homeostasis of MDA. However, MDA returned to control levels when AlDH transcript abundance was almost 10-fold higher than that of the controls, indicating successful detoxification. It is noteworthy that the relative enrichment of MDA was accompanied by decreases in LOOH (Fig. 5).

Carbohydrate profiling showed that inositol, salicin, Glc, Fru, Suc, and Gal were major osmotic compounds present in the leaves (Supplemental Figs. S4 and S5). Taken altogether, they generated a carbohydrate-induced osmotic pressure of 0.35 MPa in the leaves of the controls (Fig. 6) and their relative contributions were 39%, 38%, 8%, 7%, 7%, and 1%, respectively (data not shown). This was probably a minor fraction of the total osmotic pressure, expected to be around 1.5 MPa in such leaves (Gebre et al., 1998), other potential contributors being mineral ions, amino acids, polyamins, and polyols. Water deficit significantly increased the concentration of these carbohydrates. They generated an osmotic pressure above 0.53 MPa ($P < 0.001$) with only small changes in the relative contribution of the
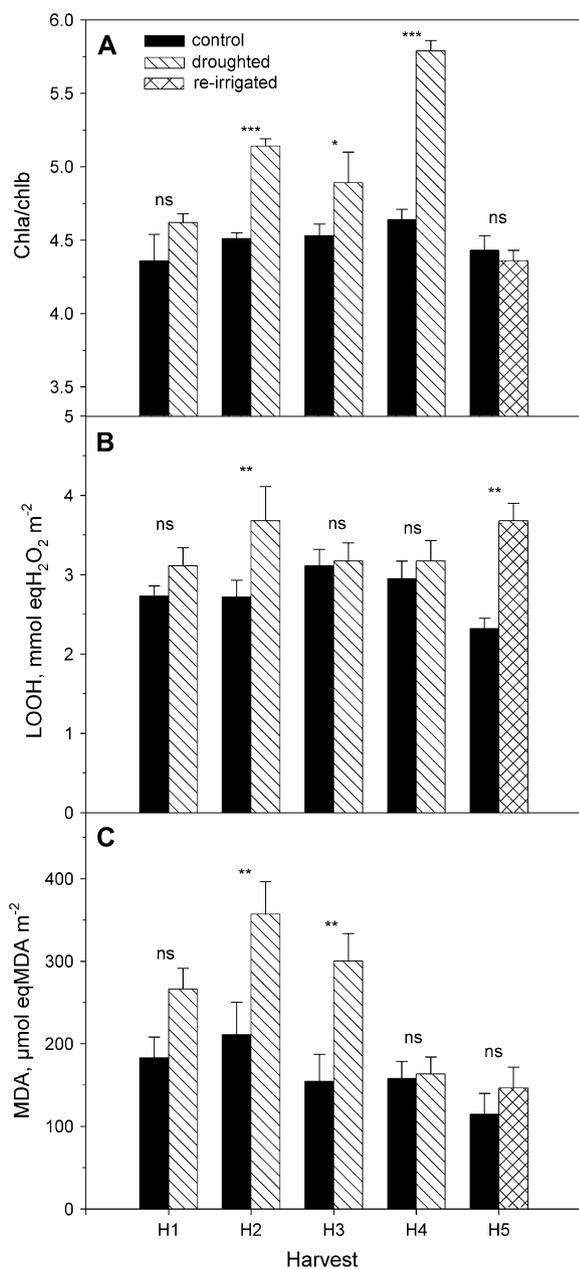
Figure 4. Chlorophyll *a*-to-chlorophyll *b* ratio (A), LOOH (B), and MDA (C) content in *P. euphratica* leaves expressed on a surface area basis at the five harvest dates. H1 to H4 correspond to four harvest dates with increasing soil water depletion and H5 to the harvest after 10 d of reirrigation. *, **, and ***, Difference was significant with $P < 0.05$, $P < 0.01$, and $P < 0.001$, respectively. ns, No significant difference.

different solutes (44%, 32%, 7%, 8%, 6%, and 3%, respectively). Increased carbohydrate content was an early response to water deficit and did not change with increasing soil water depletion. Reirrigation did not result in a return to the control value despite a slight decrease (Fig. 6). Sorbitol, mannitol, trehalose, and stachyose made a negligible contribution to osmotic pressure and were not affected or decreased slightly during water deficit (except for sorbitol and stachyose

that increased transiently at H2; Supplemental Figs. S4 and S5). Galactose and raffinose showed significant increases during water deficit despite a negligible contribution to osmotic potential (Supplemental Fig. S5). Sorbitol, mannitol, and salicin (a phenolic glucoside) remained almost completely unaffected by water deficit but increased sharply following reirrigation (Supplemental Figs. S4 and S5). There was no evidence that leaves were depleted in soluble carbohydrates, even at H4 when the net CO_2 assimilation rate had fallen to 20% of the control level (Fig. 1).

Transcriptional Response to Water Deficit

Leaf and root samples were subjected to gene expression profiling using a *P. euphratica* microarray containing 6,340 different genes (Brosché et al., 2005). Less than 1.5% of the genes on the array displayed significant changes in transcript levels at a 2-fold cutoff, 70 genes in leaves and 40 genes in roots (Fig. 7; Supplemental Tables S1 and S2). In leaves, the number of genes with changed transcript levels increased with the severity of the stress, and one-half of them were specific to harvest H4 at peak stress intensity. The expression profile in roots was very different from that of leaves. Changes occurred earlier, at lower stress intensity, and predominantly consisted of decreased transcript abundances. In both leaves and roots, most genes displaying altered expression during water deficit returned to the control levels after the plants were reirrigated and allowed to recover.

The water deficit-regulated genes were subjected to a cluster analysis to identify patterns of regulation among them (Fig. 7). In leaves, cluster A (eight genes) displayed early increases in transcript levels and a gradual increase in expression level with stress intensity (Supplemental Table S2). Among them were 1,4-α-glucan branching enzyme, thioredoxin H, alcohol dehydrogenase, and cold-regulated LTCOR12. Asn synthetase was not clustered in A but had a similar trend, with a very strong increase at H4. Cluster B (16 genes) showed increased transcript levels at harvests 3 and 4 and included cyclic nucleotide and calmodulin-regulated ion channel, putative pheophorbide a oxygenase, and a homeodomain transcription factor. Cluster C (22 genes) showed increased transcript levels only at the most severe stress level H4 and included many genes with a function in protein and sugar metabolism: Cys protease(s), trypsin inhibitors, Xyl isomerase, and Suc synthase. Genes with decreased transcript abundance fell into two clusters: D (five genes) displayed lowered transcript levels at harvests 2 to 4 and included a Pro-rich cell wall protein and an aquaporin; E (14 genes) showed a large decrease in transcript levels at harvest 4; the majority of these genes were related to photosynthesis.

Cluster analysis of transcript levels in roots identified five major clusters (Fig. 7). Cluster F (seven genes) displayed early (H1) decreased transcript abundance and included a Leu-rich repeat protein. Genes with the
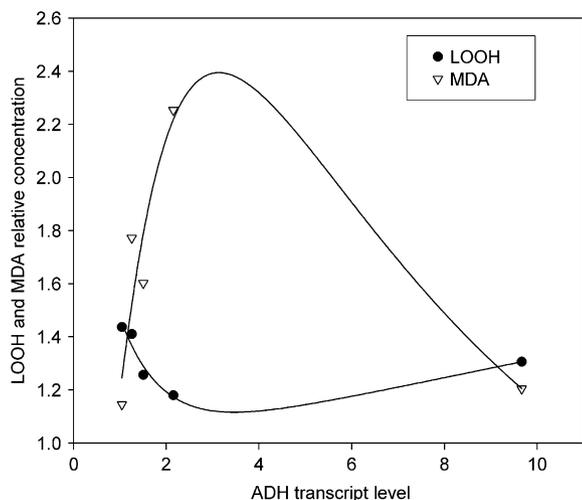
Figure 5. Correlation between relative concentrations (drought stressed versus controls) of LOOH, MDA, and AlDH transcript levels in leaves of *P. euphratica*. Log normal peak and exponential decay regression curves were fitted to LOOH and MDA, respectively.

lowest transcript level at the most severe stress intensity fell into cluster G (16 genes) and included three aquaporins (two plasma membrane intrinsic proteins [PIPs] and one tonoplast intrinsic protein [TIP]), Suc synthase, and, more strangely, genes identified as responsive to abiotic stress such PR10 protein, dehydration-responsive protein RD22, and glutathione *S*-transferase. Cluster H grouped genes with lowered transcript abundance, specifically at H2, and three of the four genes had a chaperone function, namely two heat shock proteins (HSPs) and a DNA K-type molecular chaperone. Cluster I (six genes) had increased transcript abundance, showed the highest expression level at H4 and included storage protein(s). Genes with early increased transcript levels in roots were clustered in J (seven genes), and most of them had a putative role in biotic or abiotic stress: cold-regulated LTCOR12 and drought-inducible short-chain alcohol dehydrogenase and metallothionein 2a.

Only one gene (cold-regulated LTCOR12) displayed increased, and another one (metallothionein type 2b) reduced, transcript levels in both tissues. Intriguingly, other members of the metallothionein family displayed opposite expression patterns with increased transcript levels in roots (metallothionein type 2a and 3a). Furthermore, Suc synthase increased in leaves but decreased in roots, suggesting the translocation of carbon from leaves to roots.

To validate the array results, quantitative real-time reverse transcription (RT)-PCR (qPCR) was conducted on three genes selected on the basis of different transcript level increases: no (ribosomal protein L17), moderate (calmodulin-regulated ion channel), and large (Cys protease). The RNA samples used in the DNA microarray analysis were used as templates in qPCR (Table II). For the first two genes, the expression

measured with qPCR agreed with the microarray results. Cys protease displayed a significantly higher relative expression in the qPCR analysis, but the overall response pattern was similar to that found with the microarrays. This difference probably reflects the higher dynamic range of qPCR compared to array analysis (Czechowski et al., 2004).

Protein Abundance

The abundance of individual proteins was measured in leaves by two-dimensional gels combined with fluorescent labeling (Supplemental Fig. S6). Changes in intensity were detected for 375 spots, but, in contrast to the leaf transcriptome, where the number of regulated genes increased with stress intensity, no such trend was detected for proteins (Fig. 8). Furthermore, a higher number of proteins showed changed abundance at the first harvest than at later ones. After reirrigation, the number of proteins with changed abundance increased again slightly. Among the 100 proteins tested, 39 could be identified by mass spectrometry, either by peptide mass fingerprinting (PMF) or by matrix-assisted laser-desorption ionization (MALDI)-tandem mass spectrometry (MS-MS) analysis (Supplemental Table S3). Among proteins whose abundance was higher in stressed plants, we found proteins related to energy and carbon metabolism (ATP synthase β-subunit, ATPase α-subunit; Rubisco activase, oxygen-evolving complexes involved in photosynthesis) and proteins involved in glycolysis, such as glyceraldehyde-3-P dehydrogenase and phosphoglycerate kinase. Their relative abundance (as compared to the controls) was higher at moderate stress levels and after reirrigation than at peak stress intensity. Unexpectedly, most of the proteins with decreased abundance were HSPs and
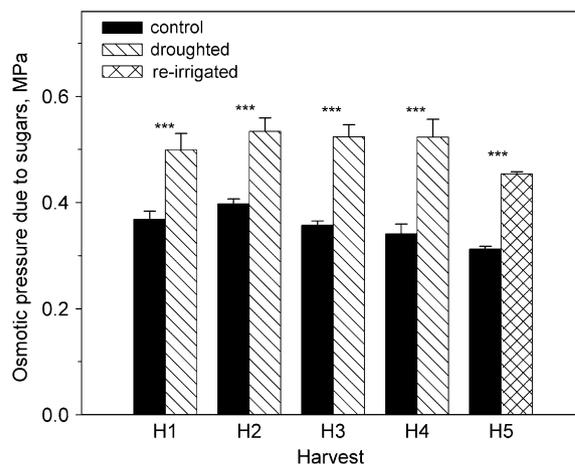
Figure 6. Full turgor osmotic pressure generated in *P. euphratica* leaves by soluble carbohydrates (megaPascal) as computed from concentrations at the five harvest dates. H1 to H4 correspond to four harvest points with increasing soil water depletion and H5 to the harvest after 10 d of reirrigation. ***, Difference was significant with $P < 0.001$.
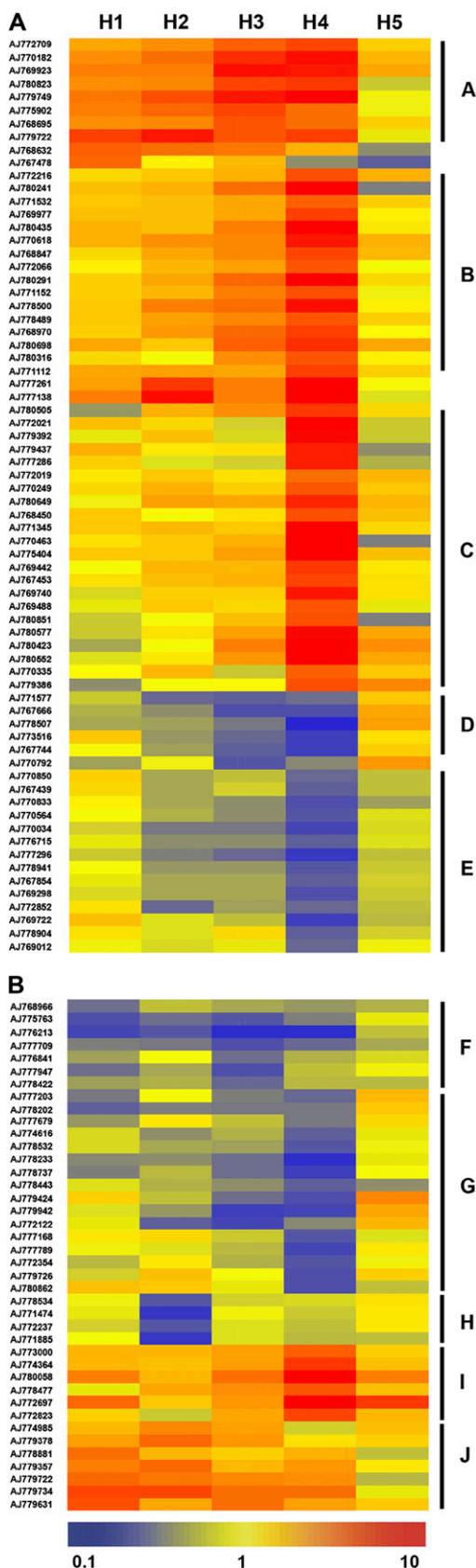
Figure 7. Differentially expressed transcripts in leaves (A) and roots (B) of *P. euphratica* during water deficit at the five harvest dates (minimum

chaperones known to be involved in stress response and defense mechanisms. Their relative abundance was more or less independent of stress intensity except for the chaperones, whose abundance was close to the control level at H2.

Stable protein-1 (SP1) was extracted from separate samples and its abundance was measured independently. SP1 is a homooligomeric protein with exceptional stability under a variety of harsh conditions, such as boiling, proteolysis, and denaturation by strong detergents and high salt concentrations (Wang et al., 2002). Similarly to chaperonins and HSP, the abundance of SP1 was decreased by water deficit (Fig. 9) and the difference between the controls and water-stressed plants was highest when stress was still moderate (H2) and decreased at peak stress intensity (H4).

Relationship between Gene Expression and Protein Abundance

For eight of the 39 proteins identified, we found a corresponding EST on the microarray. These EST-protein pairs were Rubisco activase, chloroplast glyceraldehyde-3-P dehydrogenase A, carbonate dehydratase, chloroplast phosphoglycerate kinase, cytosolic phosphoglycerate kinase, 60-kD chaperonin β-subunit, HSP 70, and cell division cycle 48. Within each pair, there was no correlation between the transcript and the protein abundance ratios (Table III). Globally, for these eight genes, the transcript ratios were close to 1 (with two exceptions), independently of harvest date, while the protein abundance ratio significantly differed from 1. Similarly, the transcript level of *sp1* did not vary despite the recorded changes in abundance of the protein SP1 (data not shown).

DISCUSSION

Transcriptome Analysis

This is the first comprehensive study, to our knowledge, encompassing a detailed characterization of whole plant performance, ecophysiology, and molecular responses to a gradually increasing water deficit and recovery, taking into account the time course and the intensity of the stress imposed on the plants. *P. euphratica*, a relatively drought-sensitive poplar species (Hukin et al., 2005), was used, and the whole response spectrum of acclimation from mild to severe water deficit was covered.

Transcriptional profiling showed that less than 1.5% of the genes on the stress-enriched EST microarray (Brosché et al., 2005) were responsive to water deficit. This is in contrast to the 30% to 35% genes that were

fold change of 2 and *P* value of 0.05). H1 to H4 correspond to four harvest dates with increasing soil water depletion and H5 to the harvest after 10 d of reirrigation. The most important clusters of transcriptional changes (A–H) are indicated. See text for details.

Table II. *Transcript abundance ratio of three genes in P. euphratica leaves measured by microarray and by qPCR at the five time points of the experiment (H1–H5)*

For the qPCR, Ct values were normalized against a glucosidase α-subunit standard to get normalized ΔCt values, which were used to calculate the fold change in expression between control and drought samples.

GenBank ID	Gene	Method	H1	H2	H3	H4	H5
AJ780423	Cys protease	Array data	0.7	1.0	2.3	13.1	1.9
		RT-PCR	4.3	31.9	266.9	600.5	7.3
AJ780698	Cyclic nucleotide and calmodulin-regulated ion channel	Array data	1.5	1.2	3.0	4.3	1.5
		RT-PCR	1.2	1.8	3.5	3.6	1.7
AJ777362	Ribosomal protein L17	Array data	1.1	1.1	1.0	0.9	1.2
		RT-PCR	1.0	1.4	0.8	1.0	1.0

reported to undergo changes at the same cutoff of 2 in response to different abiotic stresses in Arabidopsis (*Arabidopsis thaliana*; El Ouakfaoui and Miki, 2005). Nevertheless, in several other studies, a smaller fraction of genes (from 1%–10%) was regulated depending on the applied stress and on the plant organ (Kreps et al., 2002; Ozturk et al., 2002; Seki et al., 2002). In Arabidopsis, the number of regulated genes was higher shortly after stress onset (Kreps et al., 2002). Similarly, *P. euphratica* exposed to salt shock expressed a higher number of genes than after acclimation (Ottow et al., 2005). Because we focused on long-term and acclimation responses to drought in this study, genes involved in stress sensing or signaling were probably missed. Many genes identified in our study are probably involved in processes maintaining new steady states arising from decreased water availability. Several of these genes may play a role in acclimation to reduced water availability, as the intensity of the changes in transcript level increased with water deficit intensity.

Among the putative acclimation genes that showed an early response were Asn synthetase, cold-regulated LTCOR12, thioredoxin H, and alcohol dehydrogenase. Significantly increased transcript levels of a homeodomain transcription factor and RING zinc finger protein were detected at a slightly higher stress level (H2); this indicated that acclimation to water deficit also involved reprogramming of transcriptional regulation. Some of the genes regulated at harvest H4 only, i.e. under severe stress, may be related to the induction of senescence, because older leaves were shed. The pronounced induction of Asn synthetase (20-fold at this time point) suggests a strong remobilization of nitrogen before leaf senescence. The concomitant strong induction of storage proteins in roots ($\times$23 at H4) supports this suggestion. Thaumatin-like protein (osmotin), which showed increased transcript abundance at H4 in leaves, has been suggested to be induced by cell turgor loss (Bray et al., 2000). Callose synthase could be implicated in the blockage of vessels before leaf abscission. Finally, Cys protease, involved in protein catabolism and programmed cell death (Harrak et al., 2001), was also strongly induced at H4. However, changes in transcript level are not sufficient to indicate a role in water deficit acclimation, because translational and posttranslational regula-

tions largely affect the amount and activity of the corresponding proteins (Gygi et al., 1999; Kawaguchi et al., 2004).

A corresponding trend, i.e. increasing transcript levels with decreasing extractable soil water, was not found in roots. Over one-half of the regulated genes in roots were repressed, and there was no general relationship between the extent of change and soil water deficit. In both roots and leaves, reirrigation resulted in a recovery of transcripts to the control levels for most genes, showing that the observed transcriptional responses were fully reversible. For a few genes (1,4-α-glucan branching enzyme, Cys protease), significantly increased transcript levels persisted but with a lower ratio. This may be due to the inertia of the response or to a slow turnover of these mRNAs.

Proteome Analysis

In contrast to the transcriptional response in leaves, the number of proteins whose relative abundance was modified by water deficit showed no correlation with stress intensity. This could be due to the fact that, contrary to the ESTs present on the microarray that
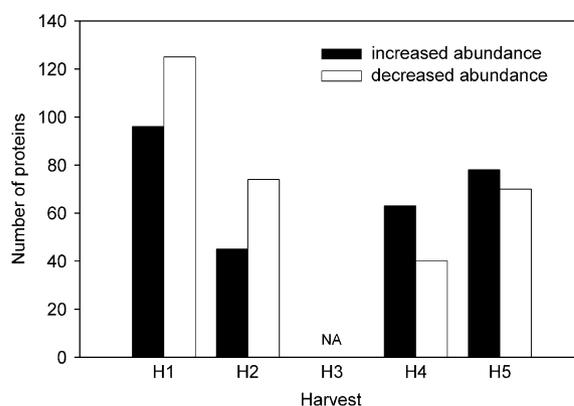
Figure 8. Number of proteins showing an increased or decreased abundance in *P. euphratica* leaves during water deficit at four harvest time dates. H1, H2, and H4 correspond to three harvests with increasing soil water depletion and H5 to the harvest after 10 d of reirrigation. NA, Not analyzed.
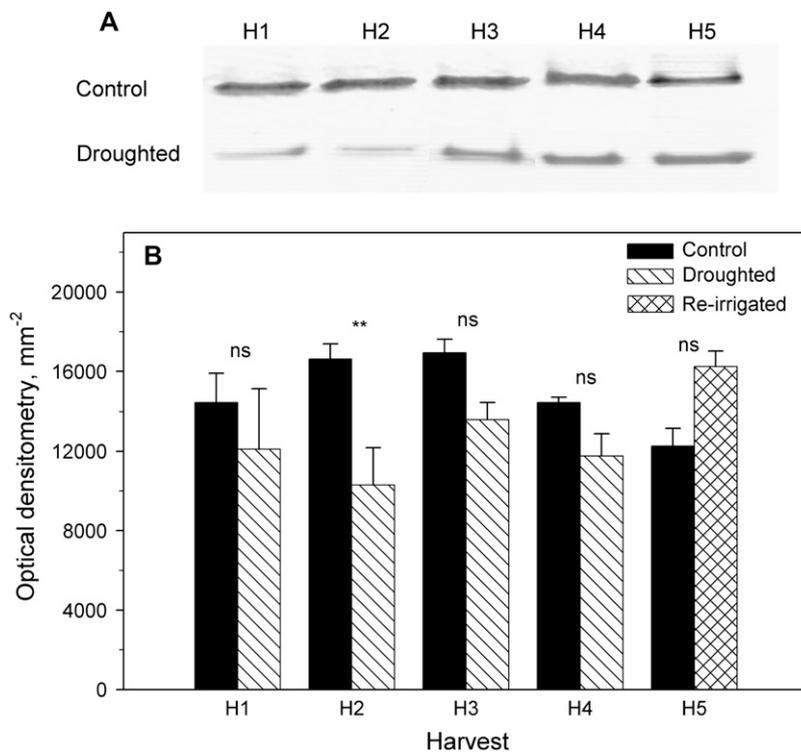
Figure 9. Abundance of SP1 proteins in *P. euphratica* leaves analyzed by SDS-PAGE analysis with Coomassie Blue staining (A; one representative sample) and by optical densitometry (B) at five harvest dates. H1 to H4 correspond to the four harvest dates with increasing water depletion and H5 to the harvest after 10 d of reirrigation. Values are means ± SE (*n* = 2–4). **, Significant difference at *P* < 0.01; ns, no significant difference.

belong to a stress-enriched collection, the proteins separated on the gel only cover soluble proteins in the pH range 4 to 7. Moreover, the analysis was also limited because proteins of low abundance were likely to be overlooked, and the results might be biased toward dominant housekeeping proteins. Among the few identified proteins for which ESTs were present on the array, no correlation between transcript level and protein abundance was found, but, as highlighted by Gygi et al. (1999), mRNAs identified by transcriptome analysis are not always translated, and, therefore, transcript and protein abundances are not necessarily linked. Recently, Kawaguchi et al. (2003, 2004) have shown that differential translational regulation makes a large contribution to the response to water deficit. Moreover, posttranslational modifications (e.g. phosphorylation, methylation, glycosylation) may further modify the apparent abundance of proteins by displacing them on the gel (Newton et al., 2004). The relative importance of changed transcription and of posttranscriptional regulation during stress responses in plants will be an important area for future studies.

Growth Reduction and Biomass Allocation in Relation to Molecular Physiology

The frequency of measurements in this study allowed the physiological perturbations induced by water deficit to be finely dissected. Growth was the most drought-sensitive process, as already described by Hsiao (1973). Stem radial growth was reduced before stem elongation, and the high sensitivity of

radial growth to drought is a well-known feature in adult trees (Breda and Granier, 1996). Growth results from cell division and cell expansion, and both processes are sensitive to water shortage (Lecoeur et al., 1995). It would be interesting to understand why secondary meristems are more sensitive to reduced water availability than primary meristems.

In the analysis of gene expression in young mature leaves, two ESTs corresponding to a Pro-rich cell wall protein showed early lowered transcript abundance with respect to the course of soil water depletion. Moreover, transcript abundance was negatively correlated to water deficit intensity, suggesting that leaf growth was also reduced. Interestingly, this gene showed significantly increased transcript abundance following reirrigation when shoot growth was resuming.

In contrast to leaf or stem growth, root growth was maintained until a low level of soil water content was reached. This change in growth allocation in favor of roots resulted in an increase of the root-to-shoot ratio, which alleviated to some extent the impairment of the plant water status through improved soil prospection at constant leaf area (Sperry et al., 2002). These water deficit-induced changes of growth allocation were accompanied by a large regulation of carbohydrate and nitrogen metabolisms, which are coregulated in higher plants (Ferrario-Mery et al., 1998). For instance, the increased transcript levels of Asn synthetase already present at mild stress levels may correspond to the shift of growth allocation from shoots to roots, because Asn is a major metabolite for nitrogen remobilization upon senescence (Dangl et al., 2000). Suc

Table III. *Protein and gene transcript abundance ratios in P. euphratica leaves for eight genes at 4/5 dates corresponding to different water deficit intensities*

H1 to H4 correspond to the four harvests with increasing water depletion and H5 to the harvest after 10 d of reirrigation. Protein AC, Protein accession number in Uniprot Database.

Protein AC	Name	Proteomics Data					Array Data					GenBank ID
		H1	H2	H3	H4	H5	H1	H2	H3	H4	H5	
Q9ATC1	Rubisco activase (fragment)	2.3	1.2		0.9	1.3	1.1	0.9	1.0	0.9	1.0	AJ780799
P12858	Glyceraldehyde-3-P dehydrogenase A, chloroplast (precursor)	2.8	1.7		1.3	2.1	1.2	0.9	1.0	1.0	0.9	AJ767436
Q41089	Carbonate dehydratase (EC 4.2.1.1) 1b	2.9	1.5		1.3	1.8	1.1	1.1	0.9	0.7	0.9	AJ767433
O82160	Chloroplast phosphoglycerate kinase	2.0	1.5		1.1	1.6	1.1	0.8	0.7	0.7	0.9	AJ769268
O82159	Cytosolic phosphoglycerate kinase 1	0.7	1.1		0.5	0.5	1.1	0.9	0.8	1.2	1.1	AJ775507
P08927	60-kD chaperonin β-subunit	0.7	0.9		0.7	0.5	1.1	1.0	1.0	1.0	1.0	AJ773373
Q9M4E6	HSP70	0.4	0.6		0.9	0.6	1.0	0.6	0.5	1.4	1.1	AJ772900
P54774	Cell division cycle 48	0.6	0.5		0.6	0.5	1.0	1.0	0.9	2.1	1.4	AJ775535

synthase was induced early in leaves and Suc concentration was increased by 25% under mild stress and by 50% under severe stress, whereas the transcript level of Suc synthase was consistently repressed in roots from the early stages of soil water depletion. The small contribution of Suc to the carbohydrate-induced osmotic potential (less than 0.03 MPa) suggests that Suc may play a role as a messenger (sugar sensing) or as a membrane/macromolecule stabilizer rather than an osmoprotectant.

Water Status in Relation to Metabolic and Transcriptional Profiles

P. euphratica is a phreatophyte species able to grow in desert areas because its roots access deep water tables (Gries et al., 2003). The occurrence of vessel embolism before stomatal closure (Hukin et al., 2005) confirmed that this species is not intrinsically drought tolerant. Thus, we expected that its capacity to acclimatize to water deficit would be limited. Although Ψ_{pd} was affected late in the time course of the experiment, Ψ_{md} and RWC were already significantly decreased at early stages of water deficit. Mild water deficit resulted in increased concentrations of soluble sugars and polyols, increasing the carbohydrate-induced osmotic pressure and thus potentially contributing to cell turgor maintenance. The osmotic adjustment capacity based on soluble carbohydrates was however, limited, because no further increases were observed, and, at maximum stress, the transcript level of thaumatin-like protein was increased; this has been suggested to be a response to turgor loss (Bray et al., 2000).

The role of aquaporins in the regulation of water relation during water deficit has been the subject of numerous studies but remains unclear (Javot and Maurel, 2002; Aharon et al., 2003; Luu and Maurel, 2005). A decreased transcript abundance of three water channel-encoding genes (two PIPs and one TIP) was recorded in roots but only at peak water deficit. A down-regulation of aquaporins by water shortage has

already been observed (Smart et al., 2001), but when all members of the PIP family of Arabidopsis were taken into account, some were up-regulated and others were markedly down-regulated by water shortage (Jang et al., 2004). The decrease of aquaporin transcripts was simultaneous to severe root growth decline. Another event occurring toward peak stress intensity was the decrease of Ψ_{pd}, indicating that leaf water status was no longer recovered during the night and that stress became severe. Thus, the decreased transcript level of aquaporins in roots could also be seen as enabling the construction of a barrier against water efflux from roots to dry soil due to reduced membrane water permeability (Smart et al., 2001).

Photosynthesis in Relation to Molecular Response

The maintenance of a high rate of net CO_2 assimilation until a relatively low extractable soil water content was reached, despite the recorded decline of stomatal conductance, allowed an increase in the instantaneous water use efficiency (A/g_s). Full or partial maintenance of photosynthesis at moderate stress levels, despite lower internal CO_2 concentrations, was accompanied by almost no transcriptional changes of photosynthesis-related genes before the most severe stress level was attained. However, it was accompanied by an increased abundance of photosynthesis-related proteins, such as oxygen-evolving complex 33-kD PSII, Rubisco activase, carbonate dehydratase (or carbonic anhydrase), chloroplast glyceraldehyde-3-P dehydrogenase, and phosphoglycerate kinase. Oxygen-evolving complex 33-kD PSII protein, an extrinsic subunit of PSII probably involved in the stabilization of the PS components (Murakami et al., 2005), was also affected under mild drought stress in spruce (*Picea abies*; Blödner et al., 2007). Rubisco activase, which regulates the activity of Rubisco in response to changes in light or temperature via ADP-to-ATP ratio and redox potential (Zhang and Portis, 1999), also accumulated in rice (*Oryza sativa*) under drought stress (Salekdeh et al., 2002). Carbonic anhydrases may be

candidates for the coregulation of mesophyll conductance and photosynthesis (Evans and von Caemmerer, 1996) and play an important role during drought and salinity stress (Flexas et al., 2004). Glyceraldehyde-3-P dehydrogenase and phosphoglycerate kinase are enzymes involved in the pentose phosphate cycle but could be impaired under drought stress (Flexas et al., 2004). This early occurrence of increased abundance of photosynthesis-related proteins during the stress treatment may have partly counterbalanced the decreased internal CO_2 concentration and contributed to the partial maintenance of photosynthesis during the first stages of water deficit. On the other hand, a putative pheophorbide a oxygenase displayed an increased transcript level (at H2). This observation is consistent with the observed increase of the chlorophyll *a*-to-chlorophyll *b* ratio, a known indication of chlorophyll catabolism when chlorophyll *b* is converted to chlorophyll *a* during senescence (Tanaka et al., 2003). At peak stress intensity, the repression of photosynthesis-related genes (Rubisco small subunit, PSI reaction center subunit VI and X) may be due to stress severity and could indicate the beginning of senescence.

Cell Homeostasis and Detoxification

The analyses of transcript, protein, and metabolite abundances showed that many enzymes or metabolites involved in cell homeostasis were regulated under soil water deficit. Among the identified regulated proteins, we found many HSPs and chaperonins, involved in protein repair and protection against denaturation, which are normally synthesized on abiotic stress exposure (Sung et al., 2001; Wang et al., 2004). For instance, a significantly higher content of chaperonin 60 (β-subunit) was found in a drought-resistant variety of sorghum, as compared with susceptible varieties, and was thought to have a positive impact on the stability of the photosynthetic components (Jagtap et al., 1998). In watermelon (*Citrullis vulgaris*), HSP70 accumulated in plants exposed to water deficit (Kawasaki et al., 2000). Surprisingly, the abundance of HSP and chaperonins were significantly decreased by water deficit in leaves of *P. euphratica*, especially at the first harvest. This may point to the inability of *P. euphratica* to activate protective processes against drought. Another reason for these contrasting results may be that our measurements were carried out after acclimation of the plant for several days to a new stress level, whereas earlier studies usually analyzed instantaneous stress responses. This idea is supported by the stress behavior of SP1, which probably has similar functions to HSP and chaperonins (Dgany et al., 2004). The *sp1* gene in *Populus tremula* plants was found to be up-regulated shortly after the application of different abiotic stresses, such as salt, cold, heat, and mannitol, but *sp1* was severely down-regulated after 24 h of exposure to mannitol (Wang et al., 2002). Similarly, the abundance of SP1 proteins was slightly reduced in water stress-acclimatized *P. euphratica* plants.

Raffinose accumulated in *P. euphratica* leaves in response to water deficit without significantly contributing to osmotic adjustment because of its low concentration. This oligosaccharide may increase drought tolerance due to its role in stabilization of membranes via interactions with phospholipid headgroups (Bentsink et al., 2000). We had no evidence of oxidative membrane degradation, and fatty acid biosynthesis appeared to be stimulated, as suggested by the elevated abundance of a putative macrolide-type polyketide synthase. Pro accumulated in leaves of *P. euphratica* in response to osmotic stress during earlier studies (Watanabe et al., 2000; Ottow et al., 2005). This is a common drought response, but, as for raffinose, the overall Pro concentrations were too low to affect cell osmotic pressure and were expected to have protective functions. It has also been suggested that compatible solutes may function as ROS scavengers (Ottow et al., 2005). The role of components such as sorbitol, mannitol, and salicin, which accumulated only after reirrigation, remains to be explained.

Metallothioneins belong to a small multigene family, of which different genes are constitutively expressed in poplar and respond differentially to environmental stimuli (Kohler et al., 2004). In addition to their role in detoxification of heavy metals, they probably contribute to cell homeostasis in response to diverse stresses (Cobbett and Goldsbrough, 2002). For instance, transcript levels of type 2 metallothionein increased in water-stressed watermelon; an increase of type 2 metallothionein was proposed to enhance scavenging of oxygen radicals (Akashi et al., 2004). In our experiment, type 2b metallothionein decreased both in leaves (late at H4) and in roots (earlier), but type 2a and 3a metallothioneins severely increased in roots only, confirming the diversity of the response of these genes.

It remains unclear how redox regulation was achieved during water deficit in our experiment. No significant changes were found in transcript or protein abundance for typical antioxidative systems such as superoxide dismutase, catalase, or other enzymes constituting typical ROS-scavenging pathways (Polle et al., 2006). Only thioredoxin transcript abundance was increased. In leaves of *P. euphratica*, typical ROS-detoxifying systems were activated during salt shock but not during long-term salinity stress, suggesting that they are required during acute stress scenarios (Ottow et al., 2005). ROS lead to the oxidation of unsaturated fatty acids in membranes, yielding LOOH (Taylor et al., 2004). These hydroperoxides are degraded nonenzymatically and cause the formation of carbonyl compounds, many of which are aldehydes (Noordermeer et al., 2000; Schneider et al., 2001). The moderate increases in MDA and LOOH were, therefore, indicating moderate oxidative stress. Moreover, MDA appeared to have been purged when transcript levels of AlDH were significantly increased. Indeed, enzymes such as alcohol dehydrogenase and AlDH have been shown to play vital roles in the detoxification

of products of lipid peroxide metabolism (Bartels and Souer, 2003). Increased transcript abundance of AlDH was also found in other plant species in response to water shortage (Ozturk et al., 2002; Bray, 2004), and its overexpression in transgenic Arabidopsis conferred higher stress tolerance (Sunkar et al., 2003).

This study provided some clues about the long-term acclimation process to soil water deficit. The reduction of shoot growth and changes of transcription levels in genes related to carbon and nitrogen metabolism were the earliest recorded responses. They occurred before other process involved in water balance maintenance, such as stomatal closure or the increase of instant water use efficiency. Most of these water deficit-induced changes were reversible, at the transcriptome as well as the whole plant level. Acclimation involved the regulation of only a small number of genes, and changes in transcription level increased with stress intensity. Different networks of genes were involved in roots and shoots. Such diverse requirements for protecting and maintaining the function of different plant organs may render plant engineering or breeding toward improved drought tolerance more complex than previously anticipated.

MATERIALS AND METHODS

Experimental Design

Plantlets of *Populus euphratica* Oliv. were multiplied by in vitro culture from tissues collected from a single mother tree originating from the desert in the Ein Avdat National Park, Israel (provided by A. Altman, Rehovot University, Israel). After ex vitro acclimation to greenhouse conditions for 6 weeks in Goettingen, plantlets were transferred to Institut National de la Recherche Agronomique Champenoux and acclimatized in a greenhouse made of fully transparent glass. After 2 weeks, they were transplanted into 7.5-L pots made from transparent Perspex tube (35 cm height, 15 cm in diameter) covered by black plastic film and filled with a peat-sand mixture (50:50, v/v). Full fertilization was provided using a slow release fertilizer (4 g L^{-1} Nutricote 13:13:13 NPK and oligonutrients). The plants were grown there for 2 months (May and June). Ambient conditions in the greenhouse depended on the external weather conditions, but the temperature was maintained in the range 15°C to 27°C with a few uncontrolled peaks (34°C), and peak irradiance varied between 400 and 1,500 μmol m^{-2} s^{-1} (cloudy versus sunny days).

Before the experiment started, batches of plants (of homogeneous size) were constituted and designated to an identified purpose. A batch of 19 plants, referred to as nondestructive measurement (NDM) plants (seven controls and 12 water-deprived plants, of which one-half were reirrigated after 25 d of water deficit), was used to monitor growth and physiological parameters nondestructively during the whole experiment: height and diameter increment, leaf emission rate, root growth, leaf water potential, net CO$_2$ assimilation, and stomatal conductance. Five other batches (of five controls and five water-stressed plants each) were designated to be harvested at five successive dates corresponding to four increasing water deficit intensities and one recovery point. These plants were moved only for monitoring the water content of the substrate. Soil water depletion evolved similarly in all batches during the course of the experiment (Supplemental Fig. S1).

Controls were watered to field capacity twice per day. A moderate and slowly increasing water deficit was applied and controlled for 4 weeks. Soil volumetric water content (SWC) was measured once or twice per day, depending on the stress intensity, by weighing the pots with a time domain reflectometry probe (Trase, Soilmoisture Equipment). For each pot, watering was withheld until SWC reached the target level (which took several days), and thereafter, controlled amounts of water were added to maintain this target SWC (±1%) for 3 d before the harvest. The target soil water contents were 10%, 7.5%, 5%, and 3%. Taking into account that the field capacity and the permanent wilting point of this substrate were close to 25% and 2% SWC, respectively, values of soil-REW were calculated as: soil-REW = (SWC − 2)/(25 − 2) × 100.

Harvest

Five control and five stressed plants were harvested at four different levels of water deficit (H1–H4; 35%, 24%, 13%, and 8% soil-REW, respectively) and after recovery (H5; 10 d at field capacity). Mature leaves and young roots were collected and frozen immediately in liquid nitrogen for transcriptome (leaves and roots) and proteome and metabolite (leaves only) analyses. A summary of the key dates of the experiment is given in Table I.

Growth Monitoring

Shoot height was recorded three to seven times per week on NDM plants. Changes in diameter of the base of the stem were continuously recorded on three controls and five water-stressed plants every 30 s with linear variable displacement transducer sensors. Root growth was monitored on the NDM plants by recording the increment of the fine root length on transparent plastic film stuck to the transparent Perspex pot twice per week. Root growth rate was calculated as the total length increment divided by the number of recorded roots and the time between two successive measurements.

Gas Exchange

g_s and net CO$_2$ assimilation rate were measured at 12 AM Universal Time, every other day on leaf 15 (a fully expanded young leaf) of all plants of the NDM batch with a portable gas exchange chamber Licor 6200 (LI-COR).

RWC and Leaf Water Potential

RWC of fully expanded nonsenescent leaves was calculated as RWC = (FW − DW)/(FTW − DW) × 100, where FW, DW, and FTW are fresh, dry, and full turgor weight, respectively. FW was measured immediately after the leaf was detached from the plant, FTW after the leaf was incubated in the dark at 4°C for 24 h with the petiole plunged in distilled water, and dry weight after the leaf was dried at 65°C for 48 h. Leaf water potential was measured on similar mature, nonsenescent leaves with a Scholander pressure bomb.

Xylem Anatomy

Measurements of the xylem anatomy were carried out on two to four plants per treatment and per harvest point. Stem segments were fixed in 2% formaldehyde, 5% acetic acid, 63% ethanol (modified after Sanderson, 1994), dehydrated in an ethanol/isopropanol series (modified after Gerlach, 1977) and embedded in Rotiplast with Roti-Histol (Roth) as the intermedium according to the manufacturer's instructions. Then, 30-μm sections were cut with a sliding microtome (Reichert-Jung) and mounted on gelatin-coated slides. The paraffin was removed with xylene, sections were stained for 15 min with Toluidine Blue (0.05% [w/v] in 0.1 M sodium acetate, pH 5.8; Merck) and examined under a microscope (Axioskop, Zeiss). Photographs were taken at 400× magnification with a digital camera (Nikon CoolPix 4500). All cells in a defined area (approximately 100 × 200 μm) containing the first fully expanded xylem cells adjacent to the cambial zone were considered. The lumen areas were measured for vessels and fibers using the image processing software analySIS (Soft Imaging System). Cell wall thickness was estimated as one-half the distance between the lumina of adjacent cells.

Microarray Analysis

Three biological replicates were used from each of the harvests with the exception of the controls of harvest 5 (only two). Each of the biological replicates contained mature nonsenescent leaves (or roots) from one or two trees. To avoid bias in the microarray evaluation as a consequence of dye-related differences in labeling efficiency and/or differences in recording fluorescence signals, dye labeling for each paired sample was reversed in two subsequent individual hybridizations. Thus, a total of six hybridizations per harvest were obtained (four hybridizations for harvest 5). The complete protocols for probe labeling and hybridization and raw data files are available from the ArrayExpress database (www.ebi.ac.uk/arrayexpress/) under the

accessions of E-MEXP-276. The production of the *P. euphratica* microarray is described in detail in Brosché et al. (2005).

Images were analyzed with GenePix-Pro 5.1 (Axon Instruments). Visually bad spots or areas on the array and low intensity spots were excluded. Low intensity spots were identified as spots where fewer than 55% of the pixels displayed an intensity above the background + 1 SD in either channel. The data from GenePix-Pro 5.1 was imported into GeneSpring 7.2 (Silicon Genetics) and normalized using the Lowess method. The background subtracted median intensities were used for calculations. Genes were selected using two criteria: (1) the gene transcript level ratio (water-stressed plants/controls) should be consistently higher than 2 or lower than 0.5 in at least one of the five harvests; and (2) the gene transcript level ratio should be significantly different from 1.0, determined using the Student's *t* test in GeneSpring. Gene trees (clustering) were drawn employing the unweighted pair-group method using arithmetic averages with genewise distances calculated by standard correlation in GeneSpring 7.2.

qPCR

The microarray results were compared with qPCR. RT was performed with 5 μg of DNase I-treated total RNA with SuperScript III according to the manufacturer's instructions (Invitrogen). The RT reaction was diluted to a final volume of 100 μL, and 1 μL was used as a template for the PCR using qPCR Mastermix Plus for SYBR Green I (Eurogentec). PCR was performed in duplicate using ABI Prism 7000 default cycling conditions (Applied Biosystems). The following primer pairs were used for PCR: Cys protease, 5'-AAGTGGGTATATGCGGATGCA, 5'-ATCCATGGCAACACCACAGA; cyclic nucleotide and calmodulin-regulated ion channel, 5'-CGTGTGTGCCA-CAGGACTTT, 5'-TGCACGTGTCGCTTATTGAGA; glucosidase II α-subunit, 5'-CTCTCATTGAGCCGGCAAAT, 5'-CCCCCCTTCAAGCATAAGG; ribosomal protein L17, 5'-GCAACATGGGTACAAAACGAGTT, 5'-CGTTTCA-GACTCCTCCTTTGAAG. The raw threshold cycle (Ct) values were normalized against glucosidase II α-subunit (shown to have a constant expression in all experiments performed on the *P. euphratica* DNA microarray) to obtain normalized ΔCt values that were then used to calculate the difference in expression levels between water-stressed and control samples.

Protein Analysis

For each harvest, three (two for harvest 5) controls were pooled into one control sample, and three drought-stressed plants were pooled into one drought sample. Proteins were extracted from 300-mg leaf samples, as described previously (Renaut et al., 2004). Dried samples were resuspended in a labeling buffer (7 M urea, 2 M thiourea, 4% CHAPS, 30 mM Tris) and incubated for 1 h at room temperature. Prior to the quantification, the pH of the solution was adjusted to 8.5. The concentration of proteins contained in the resuspended solution was then determined using a quantification kit (2D Quant kit, Amersham Biosciences).

Protein extracts and an internal standard (prepared with a pool of one-sixth of controls and stressed plants of harvests H1, H2, and H4) were labeled prior to electrophoresis with CyDyes. Three gels (corresponding to harvests H1, H2, and H4), each carrying the internal standard (Cy2), controls (Cy3), and water-stressed plants (Cy5) of the corresponding harvest, were run simultaneously. A fourth gel, carrying an internal standard (Cy2; prepared with one-half of the controls and one-half of the stressed plants of harvest H5), controls (Cy5), and drought-stressed plants (Cy3) of harvest H5, was run afterward.

A 1-nmol μL^{-1} stock solution of each dye was diluted 2:3 with anhydrous dimethyl formamide just prior to the labeling reaction. A total of 50 μg of each protein extract was mixed with 1.2 μL of Cy2, Cy3, or Cy5 (400 pmol μL^{-1}), vortexed, and incubated on ice for 30 min in the dark, as described previously by Skynner et al. (2002). The reactions were quenched by the addition of 1.2 μL of 10 mM Lys, vortexed, and incubated on ice for 10 min in the dark. An equal volume of 2$\times$ lysis buffer (7 M urea, 2 M thiourea, 4% [w/v] CHAPS, 2% dithiothreitol [DTT], and 2% [v/v] pH 4–7 immobilized pH gradient [IPG] buffer) was added. The samples were vortexed and incubated on ice for a further 15 min in the dark. Then the pooled Cy2-labeled internal standard was combined with the Cy3-labeled extracts and Cy5-labeled extracts of each batch, as described previously.

The volume of the combined labeled samples was adjusted to 450 μL with the 2$\times$ lysis buffer to dilute the samples and to avoid precipitation in the sample cup. A total of 150 μL of pooled sample (i.e. 150 μg of proteins) was loaded onto each gel and separated by electrophoresis, as indicated below.

Immobiline DryStrips (GE Healthcare, pH 4–7, 24 cm) were rehydrated overnight with rehydration buffer (7 M urea, 2 M thiourea, 1% CHAPS, 0.4% DTT, 0.5% [v/v] IPG buffers, 0.002% [v/v] bromphenol blue).

Isoelectric focusing (IEF) was carried out on an Ettan IPGphor Manifold (Amersham Biosciences) with the following settings: 100 V for 2 h, 300 V for 3 h, 1,000 V for 6 h, a gradient step up to 8,000 V during 3 h, and a constant step at 8,000 V for 4 h at 20°C with a maximum current setting of 50 μA per strip in an IPGphor IEF unit (Amersham Biosciences). After the IEF, the IPG strips were equilibrated for 15 min in equilibration buffer (50 mM Tris, pH 8.8, 6 M urea, 30% [v/v] glycerol, 2% [w/v] SDS) supplemented with 1% (w/v) DTT. A second equilibration step of 15 min with the same equilibration buffer, now containing 2.5% (w/v) iodoacetamide was carried out afterward. The IPG strips were then sealed with 0.5% agarose in SDS running buffer at the top of the gel slabs (280 $\times$ 210 $\times$ 1 mm) polymerized from 12.5% (w/v) acrylamide and 0.1% N,N'-methylenebisacrylamide. The gels were cast between low fluorescent glass plates, one treated with bind-silane. The SDS-PAGE step was performed at 15°C for 18 h in an Ettan Dalt II tank (Amersham Biosciences) using a total voltage-current energy limit of 13 W.

Cy2-, Cy3-, and Cy5-labeled protein images were produced by excitation of the gels at 488, 532, and 633 nm, respectively, and emission at 520, 590, and 680 nm, respectively, using a Typhoon Variable Mode Imager 9400 (Amersham Biosciences). Images were analyzed using the Decyder v5.02.02 software (Amersham Biosciences). The software provided automated spot detection (Differential In-gel Analysis), matching, and ratiometric quantification between the images using the Biological Variation Analysis (BVA) software (GE Healthcare). Matching of gels was facilitated by the presence of the internal standard in each gel.

Only statistically significant results were considered (Student's *t* test, $P <$ 0.05), and differentially expressed proteins with a ratio of at least 2 observed in one condition were selected using BVA.

Selected spots were located on a gel, and a picking list was generated with BVA. Spots of interest were excised from gels using the Ettan Spot Picker from the Ettan Spot Handling Workstation (Amersham Biosciences). Spots were then digested in situ with Trypsin Gold (mass spectrometry grade, Promega) using the Ettan Digester robot (Amersham Biosciences) from the same workstation, according to the manufacturer's protocols. Automated spotting of the samples was carried out with the spotter of the Ettan Spot Handling Workstation (Amersham Biosciences). Peptides dissolved in 50% acetonitrile containing 0.5% trifluoroacetic acid were spotted onto MALDI-time of flight (TOF) disposable target plates (Applied Biosystems) prior to the precoating deposit of 0.3 μL of α-cyano-4-hydroxycinnamic acid (10 mg mL^{-1}, Sigma Aldrich). Both PMF and peptide sequence analyses were carried out using MALDI-TOF/MS and MALDI-TOFTOF/MS spectra (4700 Proteomics Analyzer, Applied Biosystems). Spectral information (PMF and combined PMF and peptide sequence information) was submitted to a local search engine (Mascot V2.0, Matrix Science) and queried against the latest updates of Swiss-Prot, nrNCBI, and TrEMBL databases. The query parameters allowed for a single miscleavage, a variable oxidation state of Met, and a 50-ppm mass window resolution. For the two latter databases, taxonomic restrictions were set to *Viridiplantae*. Proteins were considered as positively identified when probability criteria exceeding 99.9% were met using the MOWSE based identification score (Perkins et al., 1999).

Comparison of EST and Protein Data

ESTs were translated in all six reading frames. For each protein identification corresponding to an EST, a multiple sequence alignment between the peptide sequence of the protein ortholog and the translated EST sequences was performed using the algorithm provided by the ClustalW WWW Service at the European Bioinformatics Institute (http://www.ebi.ac.uk/clustalw/). The translated sequence frame showing the highest score was selected for matching mass spectral data.

SP1 Protein Abundance

For each harvest, proteins were extracted from 300 mg of leaves in three or four controls and water-stressed plants chosen from the five replicates. Leaf tissue was homogenized with a chilled mortar and pestle in an extraction buffer (100 mM Tris-HCl, pH 8.5, 0.10% DTT) containing 20% of polyvinyl-polypyrrolidone per gram plant tissue. Total soluble protein samples were digested with Proteinase-K (1:4) for 1 h at 37°C. Protein samples were then boiled (100°C) for 5 min, kept on ice for another 5 min, and centrifuged 10 min at 10,000g. The supernatant fraction was precipitated by mixing it with 4 volumes of precooled acetone and kept overnight at −20°C, then centrifuged

for 10 min at 10,000g. The pellet was resuspended in diluted SDS-PAGE sample application buffer (50%, v/v). Before loading, the samples were heated at 100°C for 5 min.

Proteins were separated by SDS-PAGE in which the lower gel contained 15% polyacrylamide and the stacking gel contained 4% polyacrylamide. Each lane was loaded with 50 μg total protein, or, in the case of boiling-stable proteins, with the equivalent of 200 μg total protein, in addition to low M_r standards (kit no. SDS-7, Sigma) and run at 200 V for 45 min (on minigel). Gels were stained with Coomassie Blue stain solution (Sigma). Densitometry was measured by TINA 2.20 g Software.

Metabolite Analyses

Analyses were carried out on mature leaves of each individual plant of the five harvests (H1–H5). Concentration initially obtained in mole per gram fresh weight were converted into mole per square meter using the fresh weight-to-surface area ratio measured on another leaf sample of the same plant to avoid interference with leaf water content. For carbohydrates, concentrations were converted into mole per liter using the water content ([FW − DW]/FW) measured on another leaf sample and then into an estimate of carbohydrate-generated osmotic pressure at full turgor according to Van t'Hoff's law ($\Pi = RT \Sigma c_s$, where Π is the osmotic pressure and c_s the molarity of the osmotica at full turgor).

LOOH

LOOH concentration was measured according to DeLong et al. (2002). Plant material was ground in 80:20 ethanol:methanol (v/v) containing 0.01% (w/v) butylated hydroxytoluene (BHT). After centrifugation, the supernatant was recovered (50 μL) and added to 1 mL of a solution of 250 μM ferrous ammonium sulfate hexahydrate, 100 μM xylenol orange, and 4 mM BHT dissolved in 90% (v/v) methanol and 10% (v/v) 250 mM H_2SO_4 for 10 min at room temperature. Sample absorbance was measured at 560 nm. A standard curve was obtained using hydrogen peroxide, and the LOOH values were expressed as the hydrogen peroxide equivalent. Nonspecific turbidity was subtracted from the 560-nm signal by using the measurements at 560 nm of totally reduced samples by a prior reaction with triphenylphosphin (DeLong et al., 2002).

MDA

A modified thiobarbituric acid reactive substance assay was used as an alternative assessment of lipid oxidation (Hodges et al., 1999). Plant material was ground in 80:20 ethanol:methanol (v/v) containing 0.01% (w/v) BHT. After centrifugation, the supernatant was recovered (200 μL) and added to 1 mL of a solution of 20% (w/v) TCA and 0.01% (w/v) BHT containing 0.65% (w/v) thiobarbituric acid for 25 min at 95°C. After centrifugation, sample absorbance was measured at 532 nm. Blank measurements were performed using reagent solution without thiobarbituric acid. Nonspecific turbidity was subtracted from the 532-nm signal by using the measurements at 600 and 440 nm (Hodges et al., 1999). The results were expressed as MDA equivalent.

Pigments

Pigments were extracted from frozen leaf discs by grinding in a mortar with 2 mL acetone water (90:10; v/v) and centrifuged at 10,000g for 10 min at 4°C. The supernatant was recovered and filtered on 0.2-μm filters. Pigments were then analyzed by HPLC as described by Wright et al. (1991). HPLC separation using Photo Diode Array detection was performed on a Dionex chromatograph (Dionex) consisting of a Gina 50 autosampler, a P580 gradient pump, and a UVD340S detector. A Zorbax Bonus-RP 4.6- × 250-mm column (Agilent Technologies) was used for the pigment separation.

Carbohydrates

Soluble carbohydrate contents were determined according to Guignard et al. (2005). Samples were ground in liquid nitrogen and extracted with 80% ethanol for 1 h with gentle shaking. After centrifugation at 10,000g and 4°C for 10 min, the supernatant was dried by vacuum centrifugation at 40°C. Samples were resuspended in water prior to analysis. Ion chromatography with Pulsed Amperometric Detection analyses were carried out on a Dionex DX-500 chromatograph (Dionex) consisting of a Spark Midas autosampler, a GP-40 gradient pump, and an ED-40 electrochemical detector. Two different sets of

column and precolumn were used for carbohydrate separation. A first set, combining a Carbopac PA10 4 × 50 mm and Carbopac PA10 4 × 250 mm (Dionex) was used for the separation of common mono-, di-, and polysaccharides, while the second set combined a Carbopac MA1 4 × 50 mm and Carbopac MA1 4 × 250 mm (Dionex) and was used for the separation of sugar alcohols and trehalose.

Statistics

For the anatomy, parametric two-way ANOVA could not be used, because homoscedasticity tests failed. The differences between the controls of the five harvests were tested with a parametric one-way ANOVA for vessel lumen area and with the Kruskal-Wallis test (ANOVA on ranks) for fiber lumen area and fiber cell wall thickness. The difference between the control and water-stressed plants at each harvest was tested either with the Student's t test or the Mann-Whitney rank sum test.

For metabolites, osmotic pressure, and SP1, differences between treatments were tested with parametric two-way ANOVA, and, when significant, multiple comparison tests were made using Tukey's test.

Sequence data from this article can be found in the ArrayExpress database (www.ebi.ac.uk/arrayexpress/) under accession number E-MEXP-276.

Supplemental Data

The following materials are available in the online version of this article.

Supplemental Figure S1. Time course of SWC recorded for potted *P. euphratica* individuals during the experiment.

Supplemental Figure S2. Time course of stem diameter growth rate (A), shoot elongation rate (B), and root elongation rate (C) of *P. euphratica* during the experiment.

Supplemental Figure S3. Time course of net CO_2 assimilation rate (A) and stomatal conductance (B) of *P. euphratica* during the experiment.

Supplemental Figure S4. Inositol (A), salicin (B), sorbitol (C), mannitol (D), and trehalose (E) contents of *P. euphratica* leaves at five dates corresponding to different water deficit intensities.

Supplemental Figure S5. Gal (A), Suc (B), Glc (C), Fru (D), raffinose (E), and stachyose (F) contents of *P. euphratica* leaves at five dates corresponding to different water deficit intensities.

Supplemental Figure S6. Differential in-gel electrophoresis image.

Supplemental Table S1. Transcript abundance ratio (water-stressed to control) of 70 genes in *P. euphratica* leaves at five dates corresponding to different water deficit intensities.

Supplemental Table S2. Transcript abundance ratio (water-stressed to control) of 40 genes in *P. euphratica* roots at five dates corresponding to different water deficit intensities.

Supplemental Table S3. Relative abundance of 39 proteins (water-stressed to control) in *P. euphratica* leaves at four dates corresponding to different water deficit intensities.

LITERATURE CITED

Aharon R, Shahak Y, Wininger S, Bendov R, Kapulnik Y, Galili G (2003) Overexpression of a plasma membrane aquaporin in transgenic tobacco improves plant vigor under favorable growth conditions but not under drought or salt stress. Plant Cell **15:** 439–447

Akashi K, Nishimura N, Ishida Y, Yokota A (2004) Potent hydroxyl radical-scavenging activity of drought-induced type-2 metallothionein in wild watermelon. Biochem Biophys Res Commun 323: 72–78

Aussenac G (2000) Interactions between forest stands and microclimate: ecophysiological aspects and consequences for silviculture. Ann Sci 57: 287–301

Bartels D, Souer E (2003) Molecular responses of higher plants to dehydration. In H Hirt, K Shinozaki, eds, Topics in Current Genetics: Plant Response to Abiotic Stress, Vol 4. Springer Verlag, Heidelberg, pp 9–38

Bentsink L, Alonso-Blanco C, Vreugdenhil D, Tesnier K, Groot SPC, Koornneef M (2000) Genetic analysis of seed-soluble oligosaccharides in relation to seed storability of Arabidopsis. Plant Physiol 124: 1595–1604

Blödner C, Majcherczyk A, Kües U, Polle A (2007) Mild drought stress affects the proteome of spruce needles. Tree Physiol (in press)

Boyer JS, Cavalieri AJ, Schulze ED (1985) Control of the rate of cell enlargement: excision, wall relaxation, and growth-induced water potentials. Planta 163: 527–543

Bray EA (2004) Genes commonly regulated by water-deficit stress in Arabidopsis thaliana. J Exp Bot 55: 2331–2341

Bray EA, Bailey-Serres J, Weretilnyk E (2000) Responses to abiotic stresses. In B Buchanan, W Gruissem, R Jones, eds, Biochemistry and Molecular Biology of Plants. American Society of Plant Physiologists, Rockville, MD, pp 1158–1203

Breda N, Granier A (1996) Intra- and interannual variations of transpiration, leaf area index and radial growth of a sessile oak stand (Quercus petraea). Ann Sci For 53: 521–536

Brignolas F, Thierry C, Guerrier G, Boudouresque E (2000) Compared water deficit response of two Populus x euramericana clones, Luisa Avanzo and Dorskamp. Ann Sci 57: 261–266

Brosché M, Vinocur B, Alatalo ER, Lamminmaki A, Teichmann T, Ottow EA, Djilianov D, Afif D, Bogeat-Triboulot MB, Altman A, et al (2005) Gene expression and metabolite profiling of Populus euphratica growing in the Negev desert. Genome Biol 6: R101

Bruelheide H, Jandt U, Gries D, Thomas FM, Foetzki A, Buerkert A, Gang W, Zhang XM, Runge M (2003) Vegetation changes in a river oasis on the southern rim of the Taklamakan Desert in China between 1956 and 2000. Phytocoenologia 33: 801–818

Chaves MM, Maroco JP, Pereira JS (2003) Understanding plant responses to drought: from genes to the whole plant. Funct Plant Biol 30: 239–264

Chen SL, Li JK, Wang SS, Fritz E, Huttermann A, Altman A (2003) Effects of NaCl on shoot growth, transpiration, ion compartmentation, and transport in regenerated plants of Populus euphratica and Populus tomentosa. Can J For Res 33: 967–975

Cobbett C, Goldsbrough P (2002) Phytochelatins and metallothioneins: roles in heavy metal detoxification and homeostasis. Annu Rev Plant Biol 53: 159–182

Cosgrove D (1987) Wall relaxation and the driving forces for cell expansive growth. Plant Physiol 84: 561–564

Cosgrove DJ (2000) New genes and new biological roles for expansins. Curr Opin Plant Biol 3: 73–78

Czechowski T, Bari RP, Stitt M, Scheible WR, Udvardi MK (2004) Real-time RT-PCR profiling of over 1400 Arabidopsis transcription factors: unprecedented sensitivity reveals novel root- and shoot-specific genes. Plant J 38: 366–379

Dangl JL, Dietrich RA, Thomas H (2000) Senescence and programmed cell death. In B Buchanan, W Gruissem, R Jones, eds, Biochemistry and Molecular Biology of Plants. American Society of Plant Physiologists, Rockville, MD, pp 1044–1100

DeLong JM, Prange RK, Hodges DM, Forney CF, Bishop MC, Quilliam M (2002) Using a modified ferrous oxidation-xylenol orange (FOX) assay for detection of lipid hydroperoxides in plant tissue. J Agric Food Chem 50: 248–254

Dgany O, Gonzalez A, Sofer O, Wang WX, Zolotnitsky G, Wolf A, Shoham Y, Altman A, Wolf SG, Shoseyov O, et al (2004) The structural basis of the thermostability of SP1, a novel plant (Populus tremula) boiling stable protein. J Biol Chem 279: 51516–51523

Dreyer E, Bogeat-Triboulot MB, Le Thiec D, Guehl JM, Brignolas F, Villar M, Bastien C, Martin F, Kohler A (2004) Drought tolerance of poplars: can we expect to improve it? Biofutur 247: 54–58

El Ouakfaoui S, Miki B (2005) The stability of the Arabidopsis transcriptome in transgenic plants expressing the marker genes nptII and uidA. Plant J 41: 791–800

Evans JR, von Caemmerer S (1996) Carbon dioxide diffusion inside leaves. Plant Physiol 110: 339–346

Ferrario-Mery S, Valadier MH, Foyer CH (1998) Overexpression of nitrate reductase in tobacco delays drought-induced decreases in nitrate reductase activity and mRNA. Plant Physiol 117: 293–302

Flexas J, Bota J, Loreto F, Cornic G, Sharkey TD (2004) Diffusive and metabolic limitations to photosynthesis under drought and salinity in C-3 plants. Plant Biol 6: 269–279

Gebre GM, Tschaplinski TJ, Tuskan GA, Todd DE (1998) Clonal and seasonal differences in leaf osmotic potential and organic solutes of five hybrid poplar clones grown under field conditions. Tree Physiol 18: 645–652

Gerlach D (1977) Botanische Mikrotechnik. Georg Thieme Verlag, Stuttgart, Germany

Gries D, Zeng F, Foetzki A, Arndt SK, Bruelheide H, Thomas FM, Zhang X, Runge M (2003) Growth and water relations of Tamarix ramosissima and Populus euphratica on Taklamakan desert dunes in relation to depth to a permanent water table. Plant Cell Environ 26: 725–736

Gu RS, Liu QL, Pei D, Jiang XN (2004) Understanding saline and osmotic tolerance of Populus euphratica suspended cells. Plant Cell Tissue Organ Cult 78: 261–265

Guignard C, Jouve L, Bogeat-Triboulot MB, Dreyer E, Hausman JF, Hoffmann L (2005) Analysis of carbohydrates in plants by high performance anion-exchange chromatography coupled with electrospray mass spectometry. J Chromatogr 1085: 137–142

Gygi SP, Rochon Y, Franza BR, Aebersold R (1999) Correlation between protein and mRNA abundance in yeast. Mol Cell Biol 19: 1720–1730

Hajheidari M, Abdollahian-Noghabi M, Askari H, Heidari M, Sadeghian SY, Ober ES, Salekdeh GH (2005) Proteome analysis of sugar beet leaves under drought stress. Proteomics 5: 950–960

Harrak H, Azelmat S, Baker EN, Tabaeizadeh Z (2001) Isolation and characterization of a gene encoding a drought-induced cysteine protease in tomato (Lycopersicon esculentum). Genome 44: 368–374

Hodges DM, DeLong JM, Forney CF, Prange RK (1999) Improving the thiobarbituric acid-reactive-substances assay for estimating lipid peroxidation in plant tissues containing anthocyanin and other interfering compounds. Planta 207: 604–611

Hsiao TC (1973) Plant responses to water stress. Annu Rev Plant Physiol 24: 519–570

Hukin D, Cochard H, Dreyer E, Le Thiec D, Bogeat-Triboulot MA (2005) Cavitation vulnerability in roots and shoots: does Populus euphratica Oliv., a poplar from arid areas of Central Asia, differ from other poplar species? J Exp Bot 56: 2003–2010

Jagtap V, Bhargava S, Streb P, Feierabend J (1998) Comparative effect of water, heat and light stresses on photosynthetic reactions in Sorghum bicolor (L.) Moench. J Exp Bot 49: 1715–1721

Jang JY, Kim DG, Kim YO, Kim JS, Kang HS (2004) An expression analysis of a gene family encoding plasma membrane aquaporins in response to abiotic stresses in Arabidopsis thaliana. Plant Mol Biol 54: 713–725

Javot H, Maurel C (2002) The role of aquaporins in root water uptake. Ann Bot (Lond) 90: 301–313

Kawaguchi R, Girke T, Bray EA, Bailey-Serres J (2004) Differential mRNA translation contributes to gene regulation under non-stress and dehydration stress conditions in Arabidopsis thaliana. Plant J 38: 823–839

Kawaguchi R, Williams AJ, Bray EA, Bailey-Serres J (2003) Water-deficit-induced translational control in Nicotiana tabacum. Plant Cell Environ 26: 221–229

Kawasaki S, Miyake C, Kohchi T, Fujii S, Uchida M, Yokota A (2000) Responses of wild watermelon to drought stress: accumulation of an ArgE homologue and citrulline in leaves during water deficits. Plant Cell Physiol 41: 864–873

Kohler A, Blaudez D, Chalot M, Martin F (2004) Cloning and expression of multiple metallothioneins from hybrid poplar. New Phytol 164: 83–93

Kreps JA, Wu YJ, Chang HS, Zhu T, Wang X, Harper JF (2002) Transcriptome changes for Arabidopsis in response to salt, osmotic, and cold stress. Plant Physiol 130: 2129–2141

Lecoeur J, Wery J, Turc O, Tardieu F (1995) Expansion of pea leaves subjected to short water-deficit: cell number and cell-size are sensitive to stress at different periods of leaf development. J Exp Bot 46: 1093–1101

Luu DT, Maurel C (2005) Aquaporins in a challenging environment: molecular gears for adjusting plant water status. Plant Cell Environ 28: 85–96

Mittler R (2002) Oxidative stress, antioxidants and stress tolerance. Trends Plant Sci 7: 405–410

Monclus R, Dreyer E, Villar M, Delmotte FM, Delay D, Petit JM, Barbaroux C, Thiec D, Brechet C, Brignolas F (2006) Impact of drought on productivity and water use efficiency in 29 genotypes of *Populus deltoides x Populus nigra.* New Phytol **169:** 765–777

Murakami R, Ifuku K, Takabayashi A, Shikanai T, Endo T, Sato F (2005) Functional dissection of two *Arabidopsis* PsbO proteins. FEBS J **272:** 2165–2175

Newton RP, Brenton AG, Smith CJ, Dudley E (2004) Plant proteome analysis by mass spectrometry: principles, problems, pitfalls and recent developments. Phytochemistry **65:** 1449–1485

Noctor G, Foyer CH (1998) Simultaneous measurement of foliar glutathione, gamma-glutamylcysteine, and amino acids by high-performance liquid chromatography: comparison with two other assay methods for glutathione. Anal Biochem **264:** 98–110

Noordermeer MA, Feussner I, Kolbe A, Veldink GA, Vliegenthart JFG (2000) Oxygenation of (3Z)-alkenals to 4-hydroxy-(2E)-alkenals in plant extracts: a nonenzymatic process. Biochem Biophys Res Commun **277:** 112–116

Ottow EA, Brinker M, Teichmann T, Fritz E, Kaiser W, Brosche M, Kangasjarvi J, Jiang XN, Polle A (2005) *Populus euphratica* displays apoplastic sodium accumulation, osmotic adjustment by decreases in calcium and soluble carbohydrates, and develops leaf succulence under salt stress. Plant Physiol **139:** 1762–1772

Ozturk ZN, Talame V, Deyholos M, Michalowski CB, Galbraith DW, Gozukirmizi N, Tuberosa R, Bohnert HJ (2002) Monitoring large-scale changes in transcript abundance in drought- and salt-stressed barley. Plant Mol Biol **48:** 551–573

Passioura JB (1996) Drought and drought tolerance. Plant Growth Regul **20:** 79–83

Perkins DN, Pappin DJC, Creasy DM, Cottrell JS (1999) Probability-based protein identification by searching sequence databases using mass spectrometry data. Electrophoresis **20:** 3551–3567

Plomion C, Lalanne C, Claverol S, Meddour H, Kohler A, Bogeat-Triboulot MB, Barre A, Le Provost G, Dumazet H, Jacob D, et al (2006) Mapping the proteome of poplar and application to the discovery of drought-stress responsive proteins. Proteomics **6:** 6509–6527

Polle A, Altman A, Jiang XN (2006) Towards genetic engineering for drought tolerance in trees. *In* M Fladung, D Ewald, eds, Tree Transgenesis: Recent Developments. Springer Verlag, Berlin, pp 275–297

Renaut J, Lutts S, Hoffmann L, Hausman JF (2004) Responses of poplar to chilling temperatures: proteomic and physiological aspects. Plant Biol **6:** 81–90

Rood SB, Braatne JH, Hughes FMR (2003) Ecophysiology of riparian cottonwoods: stream flow dependency, water relations and restoration. Tree Physiol **23:** 1113–1124

Salekdeh GH, Siopongco J, Wade LJ, Ghareyazie B, Bennett J (2002) Proteomic analysis of rice leaves during drought stress and recovery. Proteomics **2:** 1131–1145

Sanderson JB (1994) Biological Microtechnique. Microscopy Handbooks 28, Royal Microscopical Society. Bios Scientific Publishers, Oxford

Schneider C, Tallman KA, Porter NA, Brash AR (2001) Two distinct pathways of formation of 4-hydroxynonenal: mechanisms of nonenzymatic transformation of the 9-and 13-hydroperoxides of linoleic acid to 4-hydroxyalkenals. J Biol Chem **276:** 20831–20838

Seki M, Narusaka M, Ishida J, Nanjo T, Fujita M, Oono Y, Kamiya A, Nakajima M, Enju A, Sakurai T, et al (2002) Monitoring the expression profiles of 7000 Arabidopsis genes under drought, cold and high-salinity stresses using a full-length cDNA microarray. Plant J **31:** 279–292

Sharma A, Dwivedi BN, Singh B, Kumar K (1999) Introduction of *Populus euphratica* in Indian semi-arid trans Gangetic plains. Ann For **7:** 1–8

Sharp RE, Poroyko V, Hejlek LG, Spollen WG, Springer GK, Bohnert HJ, Nguyen HT (2004) Root growth maintenance during water deficits: physiology to functional genomics. J Exp Bot **55:** 2343–2351

Skynner HA, Rosahl TW, Knowles MR, Salim K, Reid L, Cothliff R, McAllister G, Guest PC (2002) Alterations of stress related proteins in genetically altered mice revealed by two-dimensional differential in-gel electrophoresis analysis. Proteomics **2:** 1018–1025

Smart LB, Moskal WA, Cameron KD, Bennett AB (2001) MIP genes are down-regulated under drought stress in *Nicotiana glauca.* Plant Cell Physiol **42:** 686–693

Sperry JS, Hacke UG, Oren R, Comstock JP (2002) Water deficits and hydraulic limits to leaf water supply. Plant Cell Environ **25:** 251–263

Sung DY, Vierling E, Guy CL (2001) Comprehensive expression profile analysis of the Arabidopsis hsp70 gene family. Plant Physiol **126:** 789–800

Sunkar R, Bartels D, Kirch HH (2003) Overexpression of a stress-inducible aldehyde dehydrogenase gene from *Arabidopsis thaliana* in transgenic plants improves stress tolerance. Plant J **35:** 452–464

Tanaka R, Hirashima M, Satoh S, Tanaka A (2003) The Arabidopsis-accelerated cell death gene ACD1 is involved in oxygenation of pheophorbide a: inhibition of the pheophorbide a oxygenase activity does not lead to the ''Stay-Green'' phenotype in Arabidopsis. Plant Cell Physiol **44:** 1266–1274

Taylor NL, Day DA, Millar AH (2004) Targets of stress-induced oxidative damage in plant mitochondria and their impact on cell carbon/nitrogen metabolism. J Exp Bot **55:** 1–10

Tschaplinski TJ, Tuskan GA, Gebre GM, Todd DE (1998) Drought resistance of two hybrid *Populus* clones grown in a large-scale plantation. Tree Physiol **18:** 653–658

Tschaplinski TJ, Tuskan GA, Gunderson CA (1994) Water-stress tolerance of black and eastern cottonwood clones and four hybrid progeny. 1. Growth, water relations, and gas exchange. Can J For Res **24:** 364–371

Tuskan GA, DiFazio SP, Teichmann T (2004) Poplar genomics is getting popular: the impact of the poplar genome project on tree research. Plant Biol **6:** 2–4

Vera-Estrella R, Barkla BJ, Bohnert HJ, Pantoja O (2004) Novel regulation of aquaporins during osmotic stress. Plant Physiol **135:** 2318–2329

Vinocur B, Altman A (2005) Recent advances in engineering plant tolerance to abiotic stress: achievements and limitations. Curr Opin Biotechnol **16:** 123–132

Wang W, Pelah D, Alergand T, Shoseyov O, Altman A (2002) Characterization of SP1, a stress-responsive, boiling-soluble, homo-oligomeric protein from aspen. Plant Physiol **130:** 865–875

Wang W, Vinocur B, Shoseyov O, Altman A (2004) Role of plant heat-shock proteins and molecular chaperones in the abiotic stress response. Trends Plant Sci **9:** 244–252

Watanabe S, Kojima K, Ide Y, Sasaki S (2000) Effects of saline and osmotic stress on proline and sugar accumulation in *Populus euphratica* in vitro. Plant Cell Tissue Organ Cult **63:** 199–206

Wright SW, Jeffrey SW, Mantoura RFC, Llewellyn CA, Bjornland T, Repeta D, Welschmeyer N (1991) Improved HPLC method for the analysis of chlorophylls and carotenoids from marine-phytoplankton. Mar Ecol Prog Ser **77:** 183–196

Xiong L, Zhu JK (2002) Molecular and genetic aspects of plant responses to osmotic stress. Plant Cell Environ **25:** 131–139

Zhang N, Portis ARJ (1999) Mechanism of light regulation of Rubisco: a specific role for the larger Rubisco activase isoform involving reductive activation by thioredoxin-f. Proc Natl Acad Sci USA **96:** 9438–9443